The submitted manuscript has been created by UChicago Argonne, LLC, Operator of Argonne National Laboratory ("Argonne"). Argonne, a U.S. Department of Energy Office of Science laboratory, is operated under Contract No. DE-AC02-06CH11357. The U.S. Government retains for itself, and others acting on its behalf, a paid-up nonexclusive, irrevocable worldwide license in said article to reproduce, prepare derivative works, distribute copies to the public, and perform publicly and display publicly, by or on behalf of the Government.

ANL/APS/LS-340

New Design for a 27-mm Period Undulator for the MBA Lattice

Melike Abliz, John Grimmer, Isaac Vasserman

Abstract

By further optimizing the dimensions of a 27-mm period undulator's existing model for the MBA lattice, the magnetic force is decreased by about 28% with a gap of 11 mm. The calculated effective field with the new model was 113 G higher than the existing 27-mm period undulator, with a gap of 11 mm. The calculated field roll-off with the optimized new model is within the requirements at APS. The modeling and calculation results will be reported in detail through this paper.

Introduction

The MBA lattice will require a roughly 27-mm period undulator (instead of 33 mm) for continuous energy coverage, due to changing the electron beam's energy from 7 GeV (current energy of electron beam at APS) to 6 GeV [1]. This period undulator is therefore expected to be produced in the greatest quantities. The MBA lattice undulators will exploit an even smaller gap than the current 27-mm period undulator minimum gap of 10.5 mm, with a minimum gap as small as 9.0 mm under consideration. Various undulator magnet structure and gap separation mechanism schemes, as well as methods of swapping active magnetic structures in a single gap separation mechanism, are under consideration for use with the MBA lattice. Costs of these items can be reduced, and performance improved, by a new design that reduces the dimensions of the magnetic structure and minimizes the magnetic attractive force between opposing magnetic structures.

Modeling and Calculation Results

A quarter period undulator with a 27-mm period with the existing dimensions [2] was built with Opera 3D (as shown in Fig. 1) in order to calculate the magnetic force with it first. The magnet type N42SH from Shin-Etsu Rare Earth Magnet is set for the permanent magnet, and the pole material is set to vanadium permendur within the model. The dimensions of the magnets and poles are set the same as in the design review of this undulator magnet structure. The bh-curve of the permanent magnet is set for the temperature of 25°C, which is the same temperature at the storage ring at the APS.

The calculated B_y over the length (Z direction) with the model in Fig.1 with a gap of 11 mm is shown in Fig. 2. The effective field was calculated with the formula:

$$B_{eff} = \text{Sqrt} \left(\sum_{n=0}^{N} \frac{a_n^2}{(2n+1)^2} \right)$$
 (1)

Here, the a_n was defined by fitting the calculation data in Fig. 2 to the formula:

$$B_{y}(z) = \sum_{n=0}^{N} \left(a_{(n+1)} \sin \frac{(n+1)\pi z}{\lambda} \right)$$
 (2)

The λ here is the period length of an undulator. The calculated effective field of B_y with the existing 27-mm period undulator was 6371 G at a gap of 11 mm (Fig. 3). This field is about 4% less than the actual measured B_{eff} , which is an expected difference in line with other undulators at APS.

The calculated magnetic force in the XZ-plane with the existing 27-mm period undulator with a gap of 11 mm is shown in Fig. 4. The integrated force on the quarter-period-long undulator was 25.4 N, which means about 51 N per half period (one pole and one magnet) with the existing design. The field roll-off of the B_y field in the range of \pm 3mm in X (Fig. 5) was 4.7×10^{-4} and the maximum demagnetization field on the magnet was 15.4 kOe for the existing design as shown in Fig. 6.

The magnet and pole widths and heights are optimized with Opera 3D in the model of the 27-mm period undulator. The pole's xx and xy chamfers were optimized to get a uniform field with the new model [3]. The optimized new model is shown in Fig. 7. The widths and heights of the magnet and pole are remarkably decreased with the new model compared to the existing model. The calculated B_y vs Z with the new model is shown in Fig. 8. The effective field with the new model (Fig. 9) was 6484 G, which is about 100 G higher compared to the existing model. Also, the field roll-off of the B_y field was 6.8×10^{-4} in the range of ± 3 mm in X (Fig. 10), which is in the required order of the 10^{-4} at APS.

Figure 11 shows the calculated magnetic force over the quarter period long undulator with the new model. The integrated magnetic force at the gap center was 18.6 N, which is 37 N for a half period undulator. This is about 28% less force than the existing one. The demagnetization field on the magnet was calculated with the new model as shown in Fig. 12. The magnet's edge close to the gap showed the maximum demagnetization field of 16.6 kOe, which provides sufficient margin compared to the intrinsic demagnetization field of 21 kOe for this magnet material.

The comparison of the field parameters, magnetic force, and dimensions between the existing and new models are listed in Table 1.

Conclusion

The 27-mm period undulator was remodeled in order to investigate the possibility of decreasing the magnetic force and reducing the cost of the poles and magnets. The results show that the magnetic force will be decreased by about 28% with the new model. Additionally, the $B_{\rm eff}$ with the new model will be about 100 G higher compared to the existing 27-mm period undulator. The field roll-off in X with the new model is also within the required range. The demagnetization field with the new model is also small enough compared to the intrinsic demagnetization field of the magnet's material.

The magnet and pole of the new model are reduced by 31% and 25% in volume, respectively, compared to the existing 27-mm period undulator.

References

- [1] Michael Borland for the APS Upgrade Team, "Preliminary Expected Performance Characteristics of an APS Multi-Bend Achromat Lattice," ANL/APS/LS-337, APS, Argonne National Laboratory.
- [2] ANL Drawing #4101010203-100050 (Magnet) and #4101010203-100051 (Pole).
- [3] M. Abliz, I. Vasserman, "A Method of Optimizing Field Roll-Off and the Peak Field of Hybrid Planar Undulators," ANL/APS/LS-336, APS, Argonne National Laboratory.

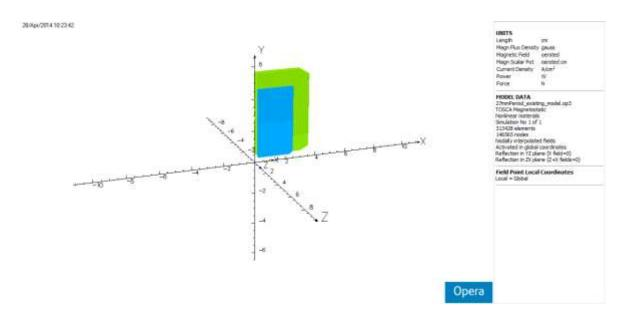


Fig. 1. A quarter part model of a quarter period length of the existing 27-mm period undulator. The green is the permanent magnet, and the blue is the pole.

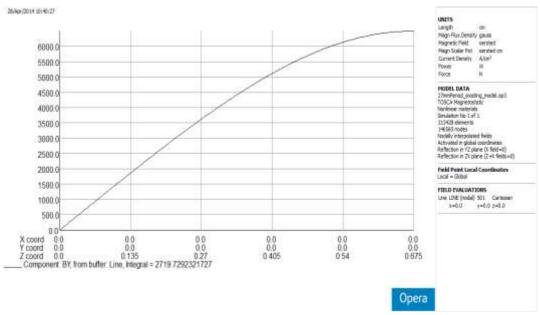


Fig. 2. Calculated field of the B_y vs Z over the quarter period long undulator of 27-mm period with a gap of 11 mm.

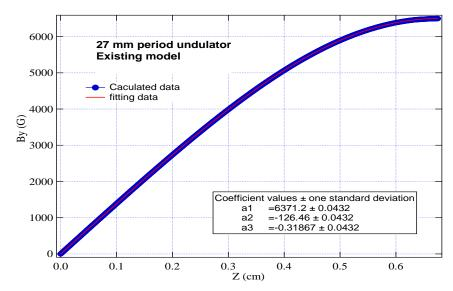


Fig.3. Fitting result to the calculated B_y vs Z over the quarter period undulator of the existing model of 27-mm period undulator with a gap of 11 mm. The blue data corresponds to the calculated field over Z, and the red line is the fitting.

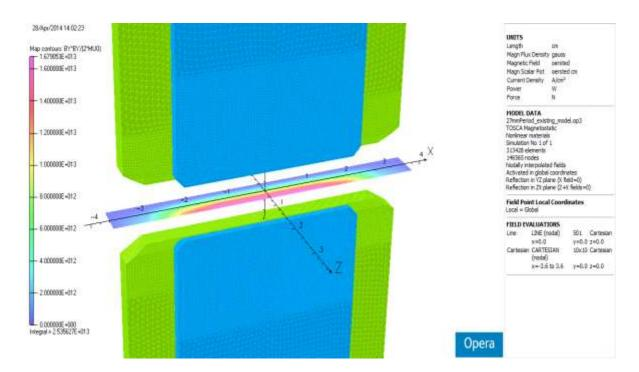


Fig. 4. The calculated magnetic force at the center of the gap with the existing model of the 27-mm period undulator with a gap of 11 mm. The color on the right shows the intensity of the calculated force.

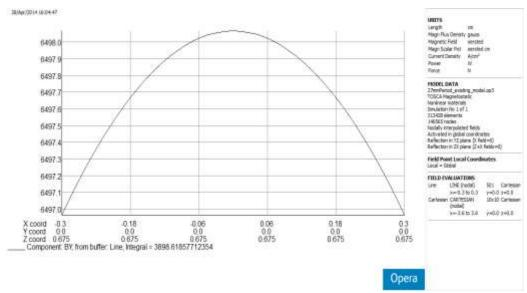


Fig. 5. Calculated B_y field over X in the range of \pm 3 mm with the model of the existing 27-mm period undulator.

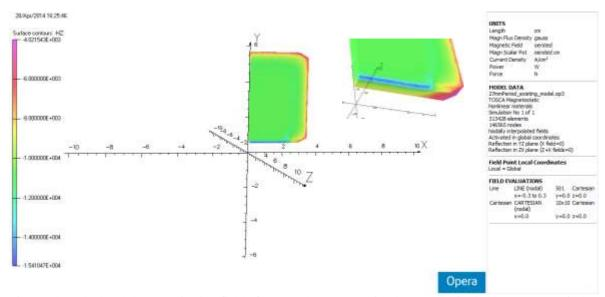


Fig. 6. The calculated demagnetization field of $-H_z$ on the magnet with the model of existing 27-mm period undulator. The dark blue on the edge close to the gap of the magnet shows the maximum demagnetization of 15.4 kOe.

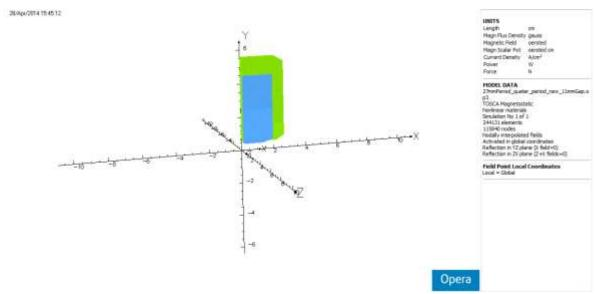


Fig. 7. New model of the 27-mm period undulator with optimized dimensions of the magnet and pole. Only a quarter part of a quarter period length of the model is shown in this figure.

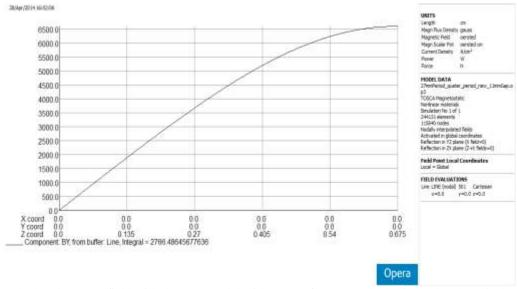


Fig. 8. Calculated B_y vs Z field with the new model with a gap of 11 mm. The horizontal and vertical axes correspond to Z and B_y in the figure.

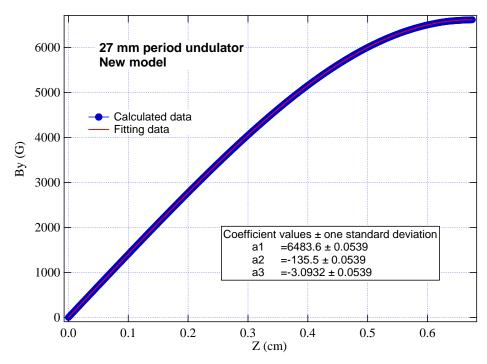


Fig. 9. Fitting result to the calculated B_y vs Z over the quarter period undulator of the new model of the 27-mm period undulator with a gap of 11 mm. The blue data corresponds to the calculated B_y field over Z, and the red line is the fitting.

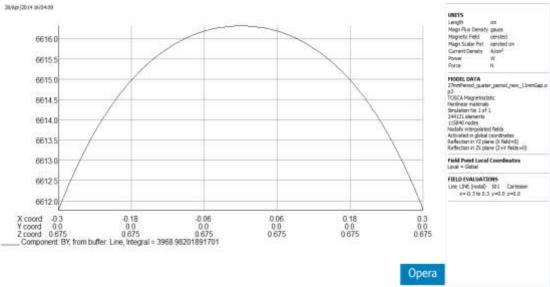


Fig. 10. Calculated B_y field over X in the range of \pm 3 mm with the optimized new model of the 27-mm period undulator.

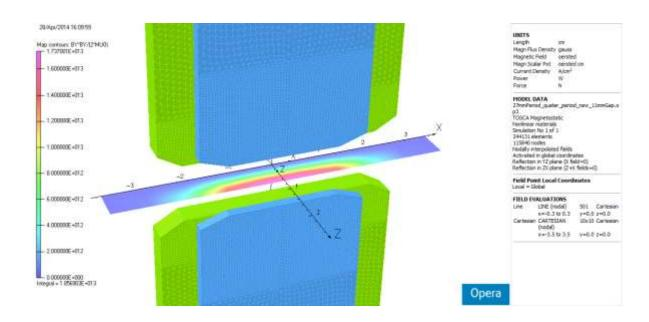


Fig. 11. The calculated magnetic force at the center of the gap with the optimized new model of the 27-mm period undulator with a gap of 11 mm. The color on the right shows the intensity of the calculated force.

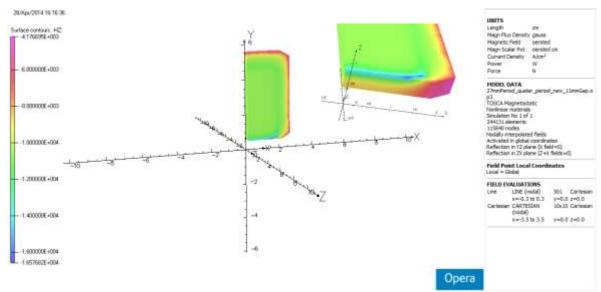


Fig. 12. The calculated demagnetization field of $-H_z$ on the magnet with the optimized new model of the 27-mm period undulator. The dark blue colored part on the edge close to the gap of the magnet shows the maximum demagnetization of 16.6 kOe.

Table 1. Comparison of magnetic forces, effective fields, demagnetization field, and dimensions between optimized and existing models of the 27-mm period undulator.

Parameters	Existing model of	New model for the
	27-mm period	27-mm period
	undulator	undulator
Beff (@11mm gap)	6371 G	6484 G
Magnetic Force (per half period)	51 N	37 N
Field roll off	5.0×10 ⁻⁴	6.8×10 ⁻⁴
Magnet length	0.915 cm	0.92 cm
Magnet width	6.70 cm	5.0 cm
Magnet height	5.41 cm	5.0 cm
Pole width	4.4 cm	3.5 cm
Pole height	4.2 cm	4.0 cm
Pole length	0.419 cm	0.425 cm
Pole's xx chamfer	0.2 cm	0.6 cm
Pole's xy chamfer	0.2 cm	0.2 cm
Magnet's xx chamfer	0.5 cm	0.5 cm
Magnet's xy chamfer	0.29 cm	0.29 cm